

Received November 10, 2020, accepted November 23, 2020, date of publication December 7, 2020, date of current version January 5, 2021.

Digital Object Identifier 10.1109/ACCESS.2020.3043013

Target Range Selection of FMCW Radar for Accurate Vital Information Extraction

HO-IK CHOI^{ID1}, HEEMANG SONG^{ID2}, (Member, IEEE),

AND HYUN-CHOOL SHIN^{ID3}, (Member, IEEE)

¹Department of Electrical Engineering, Pohang University of Science and Technology, Pohang 37673, South Korea

²Department of Electronic Engineering, Soongsil University, Seoul 156743, South Korea

³Department of Software Convergence, Soongsil University, Seoul 156743, South Korea

Corresponding author: Hyun-Chool Shin (shinhc@ssu.ac.kr)

This work was supported by the Ministry of Science and ICT (MSIT), South Korea, through the Information Technology Research Center (ITRC) Support Program, supervised by the Institute for Information & Communications Technology Planning & Evaluation (IITP) under Grant IITP-2020-2020-0-01602.

ABSTRACT Frequency modulated continuous wave (FMCW) radar, which can detect the range and small displacement of a target, has been used for contactless vital information extraction. For accurate vital sign (respiration and heartbeat) measurement, a precise selection of the target range bin, where vital information exists, is important. In this paper, an effective method for selecting the range bin with accurate vital information is proposed. The proposed method is based on the newly introduced magnitude-phase coherency (MPC) index. The experimental results show that the vital information extracted by the proposed method is more accurate than those by conventional methods, indicating that the proposed range bin selection based on MPC is an effective method for extracting accurate respiration and heartbeat rates.

INDEX TERMS FMCW radar, vital monitoring, respiration, heartbeat, range bin selection.

I. INTRODUCTION

Frequency modulated continuous wave (FMCW) radar can be used to obtain both the range and displacement information of a target [1]–[3]. The information of the range and displacement is in the spectral component of the demodulated radar signal, and the information can be simply extracted using a spectral analysis such as the discrete Fourier transform (DFT). In addition, because FMCW radar utilizes a millimeter wave, it has the advantages of low power consumption and small sized packaging [4], [5]. Owing to these properties, FMCW radar has been widely applied in various fields such as automotive control system [6], [7], gesture recognition [8], [9], structure monitoring [10], and water-level measurements [11], [12]. In biomedical applications, FMCW has been used for non-contact monitoring of vital signs (respiration and heartbeat) [1], [2], [13]–[17]. Because a non-contact vital sign monitor can operate continuously without user perception or inconveniences, it is useful for elderly home healthcare, prevention of sudden infant death

syndrome, driver monitoring systems, and search for survivors [18]–[22].

The general process of extracting vital signs from the FMCW radar signals mainly consists of spectral decomposition and range bin selection [1], [2], [13]–[17]. After the spectral decomposition using DFT, the magnitude and phase are attained at each range (or frequency) bin. The magnitude and phase at each range bin, which are called the range profile, contain the displacement information. To extract the vital signs from the range profile, it is necessary to choose a specific range bin where the vital information exists. For example, respiration can be measured within the range near the belly or chest [2], [16], and the heartbeat can be measured within the range where the skin is thin, such as the neck [23]. In conventional methods [15]–[17], the range bin is selected by exploiting either the magnitude or phase. With the method used in [15], the range bin with the maximum average magnitude, considering the reflected power from the target, is selected. In [16], the range bin with the maximum phase variation is chosen, but it is vulnerable to phase noise. In [17], range bins within a certain target range are integrated, hence vital signs may have a low accuracy. An inappropriate range bin selection results in inaccurate monitoring of vital

The associate editor coordinating the review of this manuscript and approving it for publication was Vishal Srivastava.

signs. Therefore, range bin selection is very important for the accurate detection of vital signs.

In this paper, we introduce a novel range bin selection method, that exploits the coherency between the magnitude and phase of the FMCW radar signal. Because the magnitude and the phase contain the displacement information by the respiration and heartbeat, both the magnitude and the phase need to be used to select the range bin for more accurate vital sign extraction. Based on the mathematical model and an experimental observation that the fluctuation of the magnitude and phase in the range bin where the vital signal exists are highly correlated, we devised a magnitude-phase coherency (MPC) index quantifying the coherency between the magnitude and phase in each range bin. The range bin with the maximum MPC index is then selected to extract the vital signs. In the experimental results, we demonstrate that the vital signs extracted from the proposed range bin selection are more accurate than those from conventional methods.

II. METHOD

A. FMCW RADAR SIGNAL IN VITAL DETECTION

The FMCW radar transmits a linearly modulated radio frequency signal, and receives the reflected signal from the target. The intermediate frequency (IF) signal $x(t, n)$ is then calculated by applying low-pass filtering after the mixing of the transmitted and received signals. As in (1), $x(t, n)$ is characterized by the beat frequency f_r , the magnitude $M(t, r)$, and the phase $P(t, r)$. Each component in (1) is related to the physical quantities, that is, f_r is a frequency corresponding to the range r , $M(t, r)$ is the reflected power from r , and $P(t, r)$ is the time delay of the radio signal reflected from r [1]–[3].

$$x(t, n) = \sum_r M(t, r) \cdot \cos(2\pi \cdot f_r \cdot n + P(t, r)), \quad (1)$$

where t is the scan index, n is the sample index in a chirp, r is the range, $f_r = \frac{2 \cdot BW \cdot r}{c \cdot T_c \cdot F_s}$, BW is the bandwidth, c is the speed of light, T_c is the duration of the chirp, and F_s is the sampling frequency.

DFT is used to extract $M(t, r)$ and $P(t, r)$ from $x(t, n)$, as in (2).

$$\begin{aligned} X(t, r_k) &= \sum_{n=0}^{N-1} x(t, n) \cdot \exp\left(-\frac{j \cdot 2\pi \cdot k \cdot n}{N}\right), \\ M(t, r_k) &= 2|X(t, r_k)|, \\ P(t, r_k) &= \angle X(t, r_k), \end{aligned} \quad (2)$$

where $r_k = \frac{c}{2BW} \cdot k$ for $k = 0, \dots, N - 1$.

When an object exists in r_k , $M(t, r_k)$ and $P(t, r_k)$ are modeled as in (3) [1]–[3], [24], [25].

$$\begin{aligned} M(t, r_k) &= \frac{M_0}{4\pi \cdot r_k^2}, \\ P(t, r_k) &= \frac{4\pi \cdot f_c}{c} \cdot r_k, \end{aligned} \quad (3)$$

where M_0 is the magnitude of the transmitted radio signal, and f_c is the center frequency.

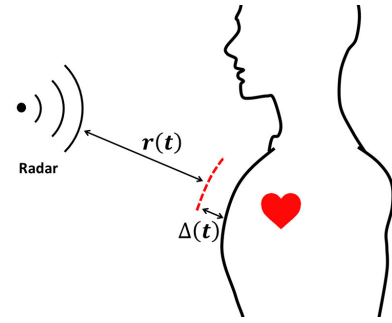


FIGURE 1. Radar and target with vital displacement.

Suppose that the object in r_k moves with the small displacement $\Delta(t)$ as

$$r(t) = r_k + \Delta(t). \quad (4)$$

Then, replacing r_k in (3) with (4), (3) is changed to

$$\begin{aligned} M(t, r_k) &= \frac{M_0}{4\pi \cdot (r_k + \Delta(t))^2} \\ P(t, r_k) &= \frac{4\pi \cdot f_c}{c} \cdot (r_k + \Delta(t)). \end{aligned} \quad (5)$$

In addition, assuming $|\Delta(t)| \ll r_k$, $M(t, r_k)$ in (5) is approximated by Taylor series [26] as

$$M(t, r_k) \approx \frac{M_0}{4\pi \cdot r_k^2} \cdot \left(1 - 2 \frac{\Delta(t)}{r_k}\right). \quad (6)$$

As shown in (5) and (6), the small displacement, $\Delta(t)$ in r_k is reflected in both the magnitude, $M(t, r_k)$ and the phase, $P(t, r_k)$, and moreover the magnitude and the phase are linearly proportional to the small displacement. Thus, by exploiting $M(t, r_k)$ and $P(t, r_k)$, we can measure the displacement, $\Delta(t)$. In the case of measuring the vital signs, $\Delta(t)$ is the body displacement caused by the respiration and heartbeat, as depicted in Fig.1.

Fig.2 shows the result of the respiration and heartbeat extraction from a single subject. Fig.2a shows the $M(t, r)$ and $P(t, r)$ for respiration. In Fig.2c, $M(t, r)$ and $P(t, r)$ of Fig.2a in several range bins are shown. $M(t, r = 0.700m)$ and $P(t, r = 0.700m)$ are proportional to the referenced respiration signal. However, for $r = 0.550m$ or $1.100m$, the $M(t, r)$ and $P(t, r)$ are not associated with the referenced signal. Likewise, Fig.2b,d show the result for the heartbeat. In Fig.2d, $M(t, r = 1.200m)$ and $P(t, r = 1.200m)$ are highly correlated to the referenced heartbeat signal. However, for $r = 1.025m$ or $1.325m$, $M(t, r)$ and $P(t, r)$ have no association with the referenced signal. That is, in some range bins, $M(t, r)$ and $P(t, r)$ are proportional to the respiration or heartbeat signal. However, other range bins are not related to the respiration or heartbeat. Thus, for accurate extraction of the respiration and heartbeat information, a precise range bin selection is necessary.

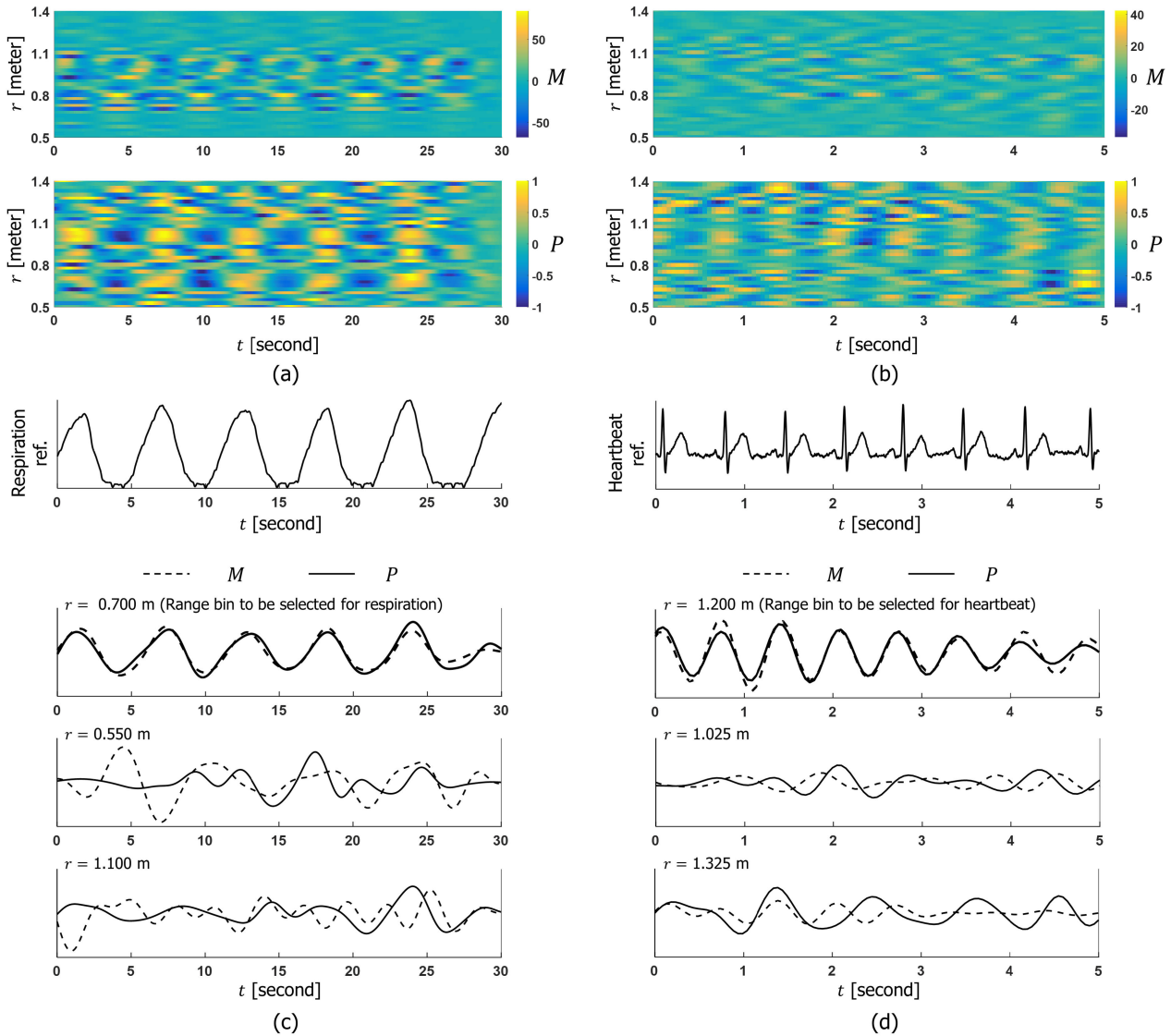


FIGURE 2. Respiration and heartbeat in various range bins. (a), (b) $M(t, r)$ and $P(t, r)$ for respiration and heartbeat, and (c), (d) referenced signal and extracted respiration and heartbeat.

B. PROPOSED RANGE BIN SELECTION

To select the range bin with accurate vital information, we introduce a novel range selection method utilizing the coherency between $M(t, r)$ and $P(t, r)$. As shown in (5),(6) and Fig.2, both $M(t, r)$ and $P(t, r)$ in range bin r_k , where an accurate respiration or heartbeat is contained, are proportional to the displacement by the respiration and heartbeat. Thus, $M(t, r)$ and $P(t, r)$ in r_k are highly correlated and the coherency between $M(t, r)$ and $P(t, r)$ is expected to be high. To quantify the coherency, we devise the MPC index as

$$MPC(t, r) = \frac{\left| \sum_{s=t-t_0}^t M(s, r) \cdot P(s, r) \right|}{\sigma_M(r) \cdot \sigma_P(r)}, \quad (7)$$

where the temporal means of $M(t, r)$ and $P(t, r)$ are removed in advance, and $\sigma_M(r)$ and $\sigma_P(r)$ are the standard deviation of $M(t, r)$ and $P(t, r)$, respectively.

We then select the range bin with the highest MPC value for the vital target $r_T(t)$ as in (8).

$$r_T(t) = \arg \max_r MPC(t, r). \quad (8)$$

To see how well MPC reflects the coherency between $M(t, r)$ and $P(t, r)$, we tested MPC with simulated data in Fig.3. $M(t, r)$ in Fig.3a does not change for the range, but $P(t, r)$ becomes gradually disordered from r_1 to r_7 . As the coherency between $M(t, r)$ and $P(t, r)$ decreases from r_1 to r_7 , MPC also decreases, as shown in Fig.3b.

In addition, to check the efficacy of MPC for selecting the range bin with vital information, we tested MPC with real FMCW radar signals. In Fig.4a,b, MPCs for various range bins are shown. Fig.4c,d show the referenced and extracted respiration. As can be seen in Fig.4c, the extracted respiration in the range bins ($r = r_{R2}, r_{R1}$), where MPCs are

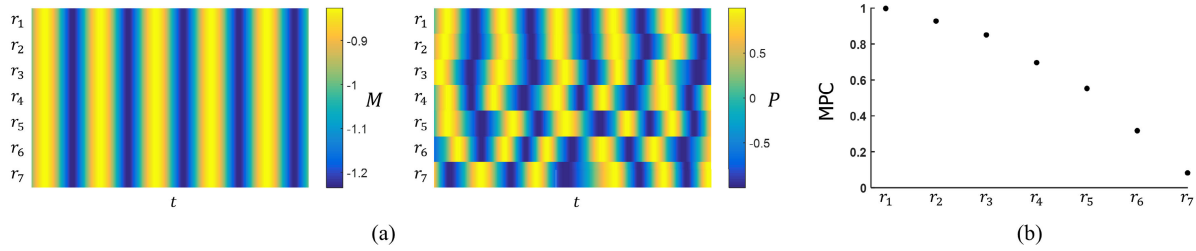


FIGURE 3. Simulated test of MPC. (a) Generated $M(t, r)$ and $P(t, r)$, and (b) MPC.

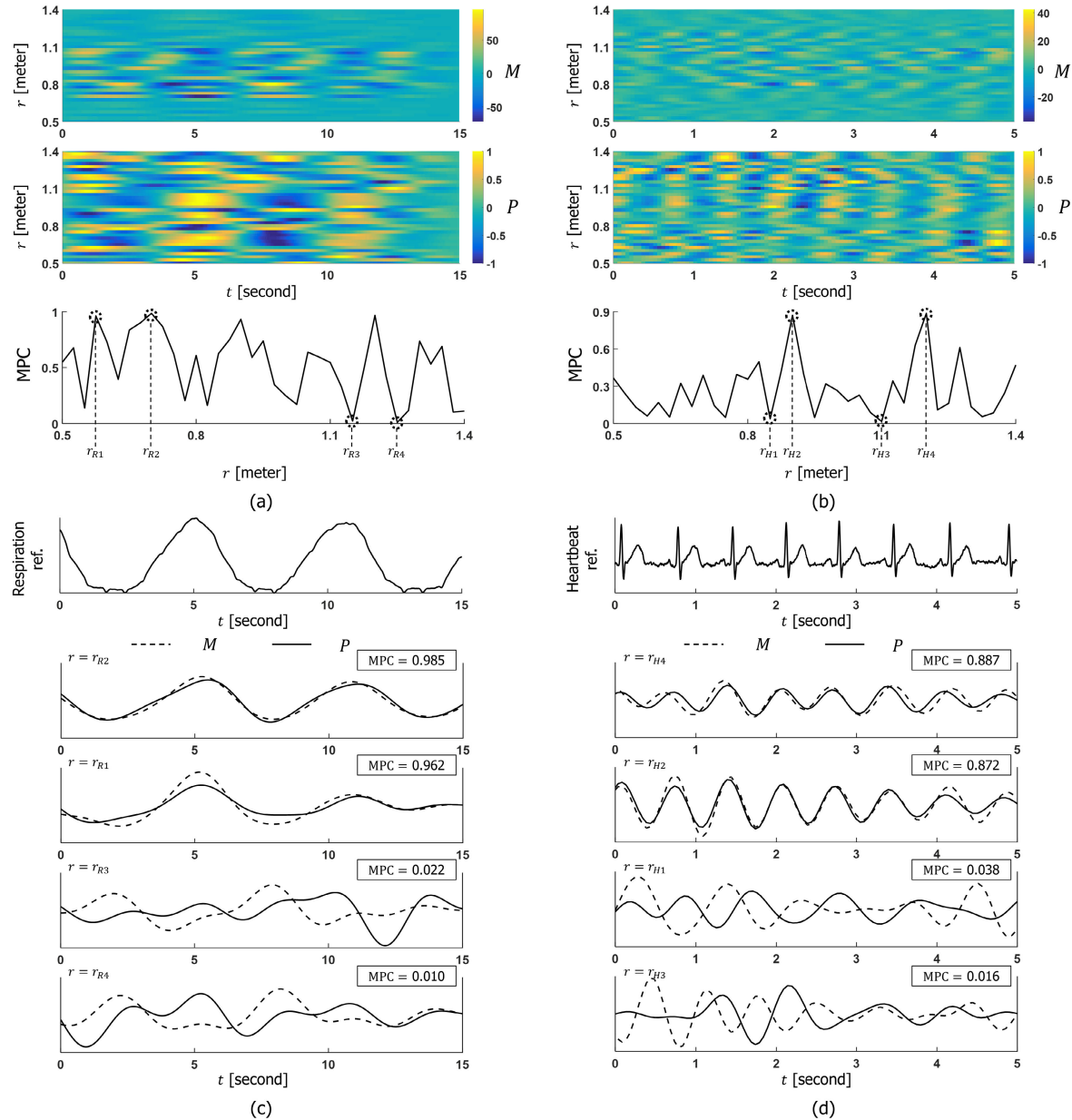


FIGURE 4. MPC and extracted vital signs (respiration and heartbeat) for various range bins. (a), (b) MPCs for respiration and heartbeat, and (c), (d) referenced and extracted vital signs.

high, are proportional to the referenced respiration. However, the extracted respiration in the range bins ($r = r_{R3}, r_{R4}$), where MPCs are low, are not correlated with the referenced

respiration. Similarly, in Fig.4d, the extracted heartbeat in the range bins ($r = r_{H4}, r_{H2}$), where the MPCs are high, are proportional to the referenced heartbeat. However, the extracted

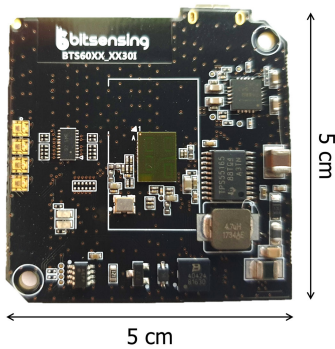


FIGURE 5. FMCW radar.

TABLE 1. Radar parameters and specifications.

Parameter	Symbol	Value
Center frequency	f_c	61 GHz
Bandwidth	BW	6 GHz
Chirp duration	T_c	128 μ s
Sampling frequency	F_s	2 MHz
Scan interval	-	50 ms
Tx antenna	-	1 channel
Rx antenna	-	3 channel
Beamwidth (Azimuth)	-	$\pm 65^\circ$
Beamwidth (Elevation)	-	$\pm 65^\circ$

heartbeat in the range bins ($r = r_{H1}, r_{H3}$), where the MPCs are low, have no correlation with the referenced heartbeat.

In summary, the accuracy of the extracted vital signs depends highly on the selection of the range bin. By choosing the range bin with the maximum MPC, we can select the range bin for extracting the accurate vital signs.

III. RESULT

A. RADAR RECORDING

We selected 18 volunteers with normal respiration and heart-beat rate. All subjects were well informed about the whole process of the experiment, and took a rest at least 5 min before the vital measurement. The FMCW radar used in the experiment was BTS60 (bitsensing INC. Korea) [27] shown in Fig.5, and the parameters were set as in Table.1. Among the 3 Rx channels of radar, we used the channel 1. The referenced respiration was measured using Neulog Respiration Monitor Belt logger sensor (Neulog INC. Israel), and the ECG of the referenced heartbeat was measured using PolyG-A (Laxtha INC. Korea). Fig.6 shows the experimental setting for the vital measurements. The radar was set in front of the subjects. The subjects sat on a chair at 1.0m from the radar, and the measurement lasted for 2min for each subject. One of the subjects repeated the measurement changing the location from 0.4 to 1.4m.

B. PROCESSING

To prevent spectral distortion, the Hamming window function was applied to $x(t, n)$ before the DFT. A 15s interval



FIGURE 6. Experimental setting for the vital measurement.

of $x(t, n)$ was used as an epoch for the vital sign analysis, that is, $t_0=15$ s, and each epoch was calculated every 1s for the time continuity. For the reduction of computational complexity, the candidate of the range bins, where a human target exists, was detected by [28]. Then, $M(t, r)$ and $P(t, r)$ in each detected range bin are filtered for the respiration (0.1-0.4Hz) and heartbeat (0.8-1.7Hz) band, considering the normal bounds of an adult's respiration and heartbeat frequency [29], [30]. Next, the MPCs were calculated using $M(t, r)$ and $P(t, r)$ for the respiration and heartbeat. Although, both $M(t, r)$ and $P(t, r)$ contain displacement information, $M(t, r)$, which comes with higher-order harmonics, is less robust for measuring vital signs than $P(t, r)$ [31]. Therefore, we utilized $M(t, r)$ for the calculation of MPC, and extracted the vital rates from $P(t, r)$. Zero-crossing detection [32], [33] was used to count the respiration and heartbeat in $P(t, r)$ as well as the referenced signals. For comparison with the conventional range selection methods [15]-[17], other processes were applied in the same way as the proposed method, and only the range bins were selected by the conventional methods. We then compared the vital signs extracted by the proposed with those by conventional methods.

C. ACCURACY ANALYSIS

We examined the accuracy of the vital signs extracted by the proposed range bin selection method. Fig.7 and 8 show the results of the range bin selections for two single subjects at fixed distance. Fig.7a,b and Fig.8a,b show $M(t, r)$ and $P(t, r)$ for the respiration and heartbeat, respectively. Fig.7c,d and Fig.8c,d compare the vital signs extracted by the proposed and conventional methods. The respiration and heartbeat extracted by the proposed method are highly correlated with the referenced signals for both subjects whereas the vital signs extracted by the conventional methods are not. Fig.7e,f and Fig.8e,f show $r_T(t)$, and the respiration and heartbeat rates of the proposed and conventional methods, respectively. Both the respiration and heartbeat rate of the proposed method are consistent with the referenced respiration and heartbeat rate. But the respiration and heartbeat rate of the conventional methods often deviate from the referenced vital

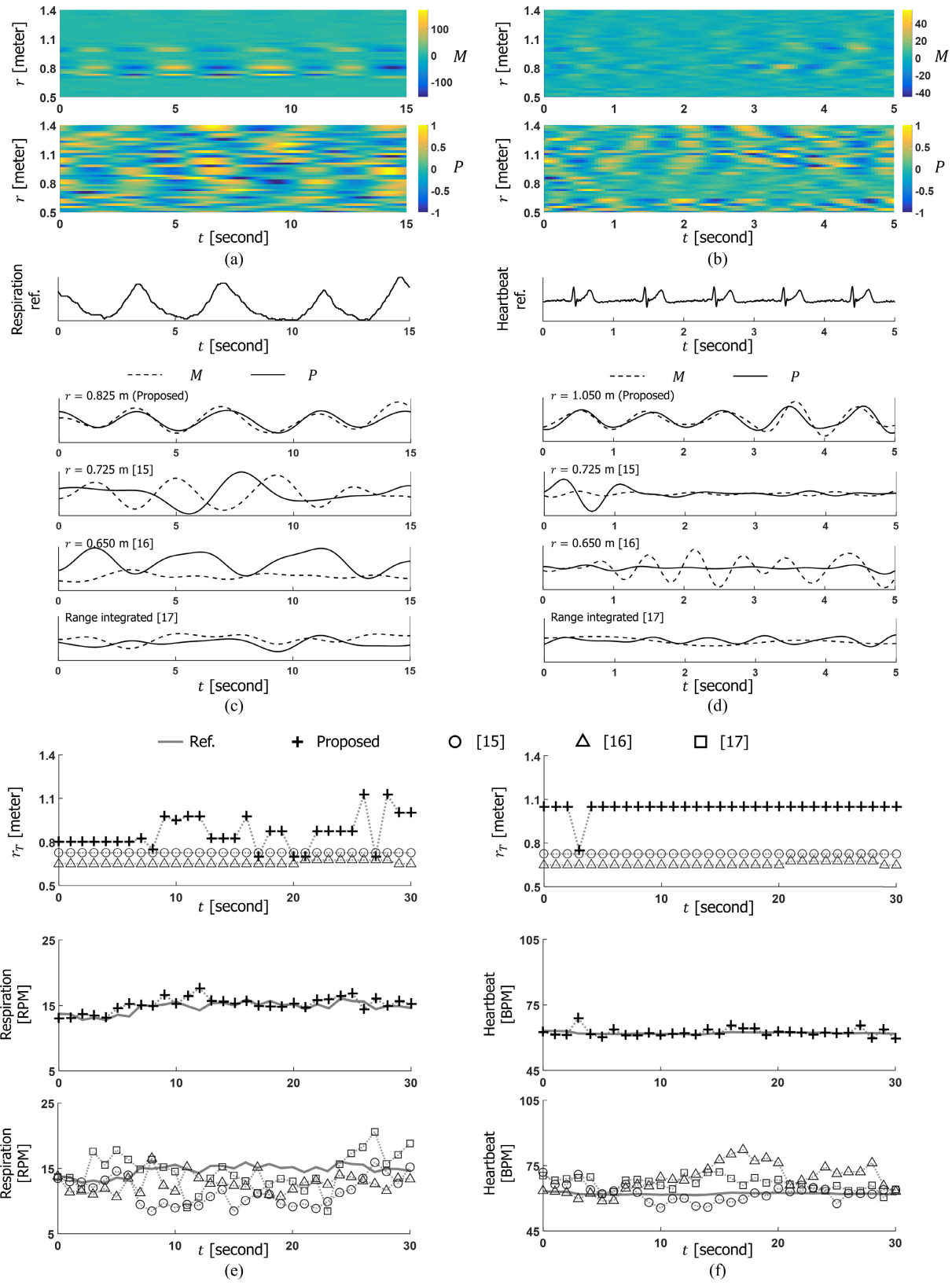


FIGURE 7. Results of the vital sign (respiration and heartbeat) extraction for a subject. (a), (b) $M(t, r)$ and $P(t, r)$ for respiration and heartbeat, (c), (d) referenced and extracted vital signs, and (e), (f) $r_T(t)$ and vital rates of the proposed and conventional methods.

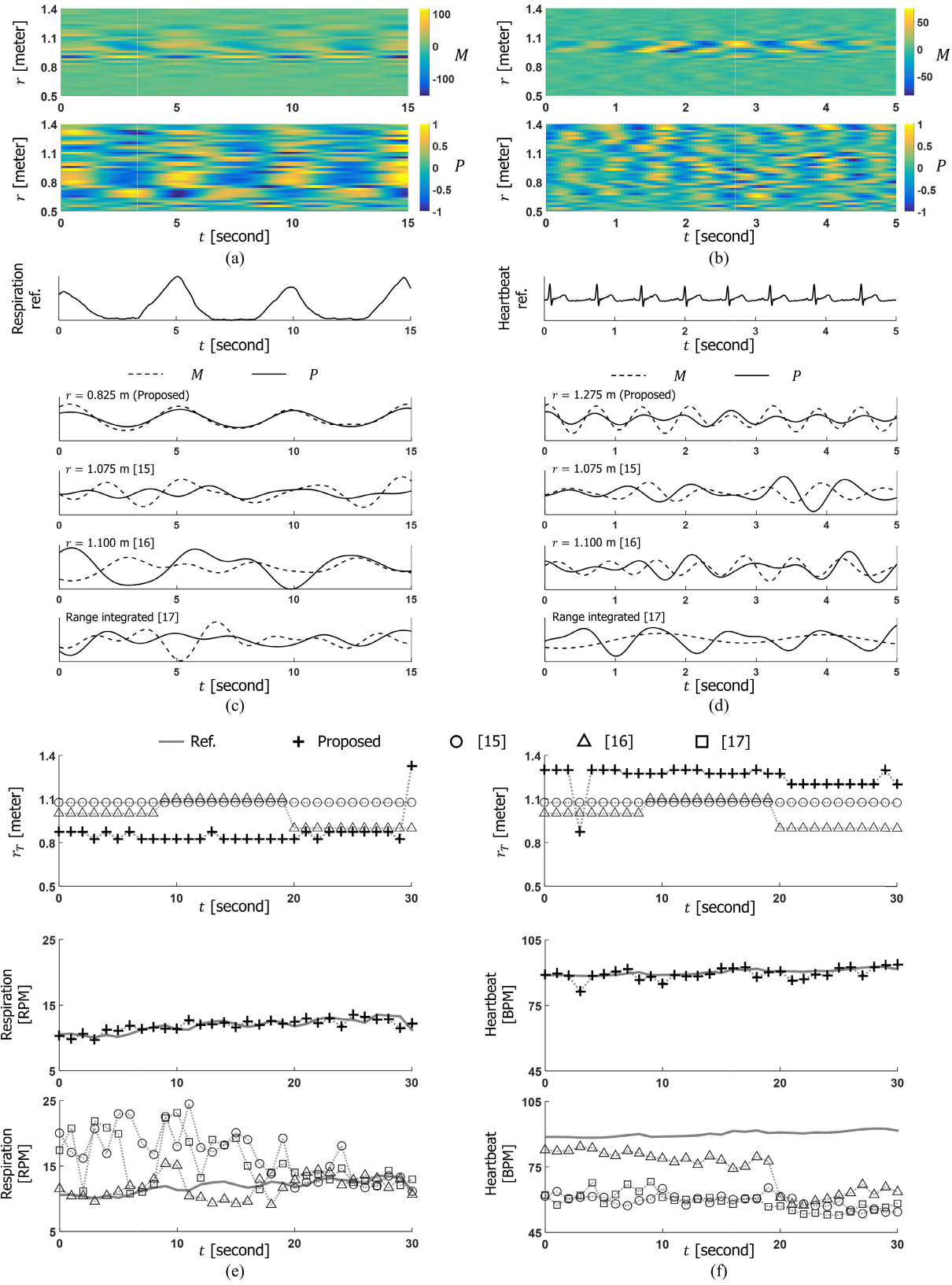


FIGURE 8. Results of the vital sign (respiration and heartbeat) extraction for another subject. (a), (b) $M(t, r)$ and $P(t, r)$ for respiration and heartbeat, (c), (d) referenced and extracted vital signs, and (e), (f) $r_T(t)$ and vital rates of the proposed and conventional methods.

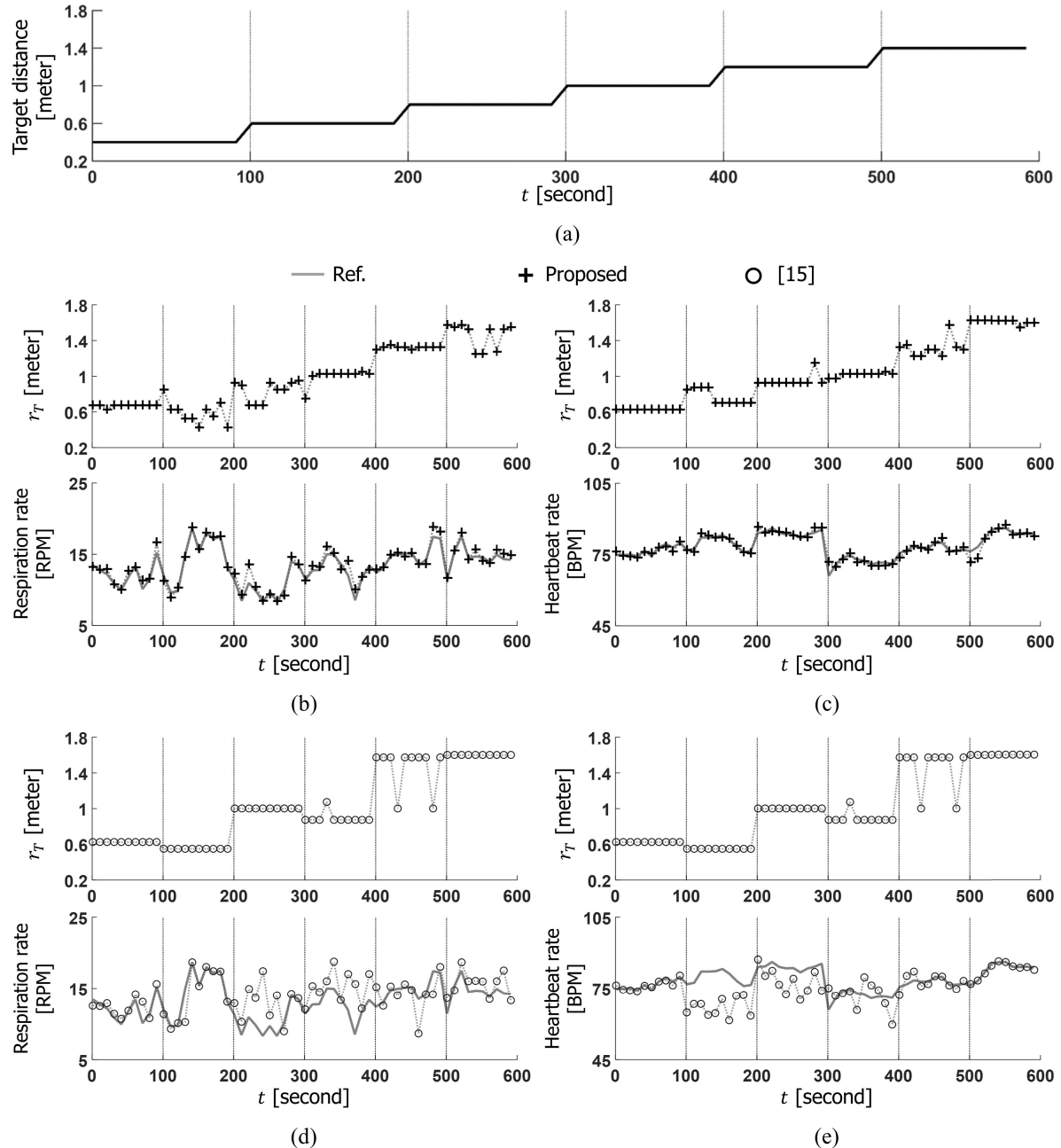


FIGURE 9. Estimated vital rate, when the location of the target changes. (a) Target location, (b), (c) $r_T(t)$ and vital rates of the proposed method, and (d), (e) $r_T(t)$ and vital rates of the method in [15].

rates. In Fig. 7e, though range bins selected by the proposed method fluctuate from 0.8 to 1.1m, the respiration information can be extracted from range bins apart 0.3m from each other considering that belly and chest are more than 0.3m apart. In addition, at close to $t=20$ s, although the range bins selected by the proposed (0.700m) and conventional ([15]: 0.725m, [16]: 0.650m) methods are close, the respiration rates by these methods are differed. The proposed method is more accurate than the conventional methods.

Fig. 9 shows $r_T(t)$ and the extracted vital rates of the proposed method and the conventional one in [15], when the location of the subject is changed. Because accuracy of the method in [15] was highest among the conventional methods in our experimental results (Table.2), we compared the proposed method only with the method in [15] as a representative. The vital rates extracted by the proposed method are consistent with the referenced vital rates as shown in Fig. 9b,c. However, the respiration and heartbeat rate extracted by [15]

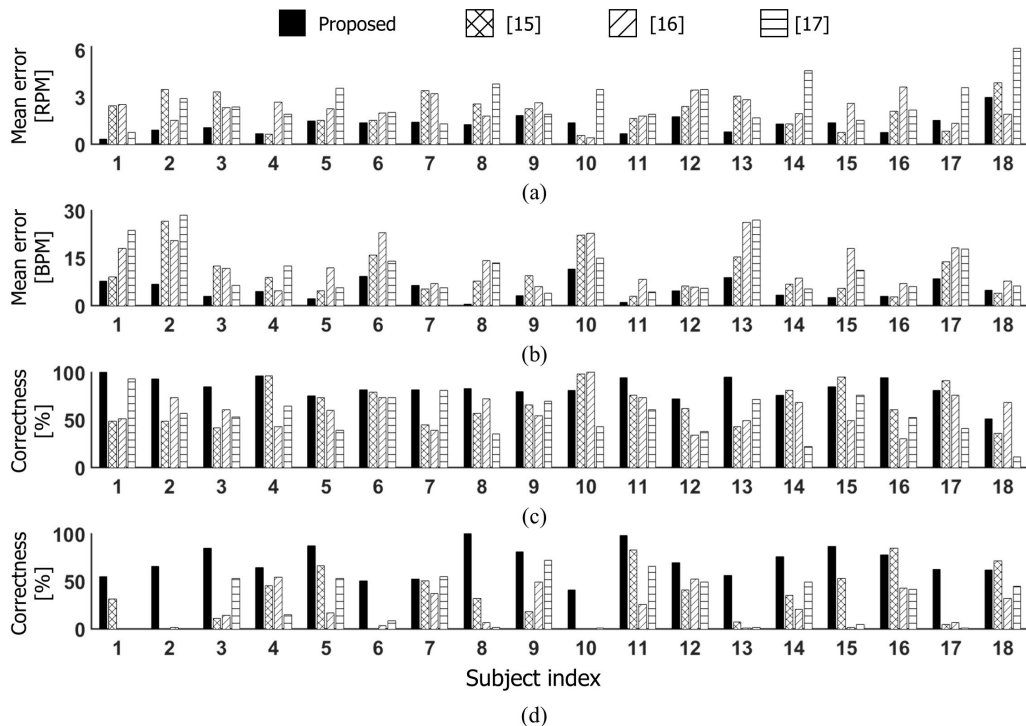


FIGURE 10. Accuracy of vital (respiration and heartbeat) rates. (a), (b) Mean error of respiration and heartbeat rate, and (c), (d) correctness of respiration and heartbeat rate.

TABLE 2. Accuracy of vital rates.

	Method	Error	Correctness [%]
Respiration	Proposed	1.27	83.7
	[15]	2.09	66.6
	[16]	2.27	59.9
	[17]	2.73	54.6
Heartbeat	Proposed	5.14	70.7
	[15]	9.99	35.4
	[16]	13.34	20.5
	[17]	11.80	28.9

have an error at some time points as shown in Fig.9d,e. The result demonstrates that the proposed method can extract the vital information accurately even under the change of the subject's location.

In addition, we calculated the mean error, and the correctness of the estimated vital rates measured for 18 subjects. The mean error is the absolute difference between the referenced and estimated vital rates. The correctness [17] is the ratio of the estimated vital rates within a difference of 2 RPM for the respiration rate, and 5 BPM for the heartbeat rate. Fig.10 shows the mean error and correctness of the vital rates for each subject. For most of the subjects, the mean error of the proposed method is lower, and the correctness of the proposed method is higher than those of conventional methods. Furthermore, unlike the mean error and the correctness of the conventional methods, which are largely differed by the subjects, the mean error and the correctness of the proposed method have less variation for the subjects. Table. 2 show the

average of the mean error and the correctness of all subjects for respiration and heartbeat. Overall, the proposed method has a lower mean error, and higher correctness of the vital rates than conventional methods.

IV. CONCLUSION

The accuracy of the vital signs depends highly on the range bin selection. For accurate vital measurements, we selected the range bin based on the newly introduced MPC. We experimentally showed that the range bin selection based on MPC results in accurate vital information extraction. In experimental results, we analyzed the radar recordings of 18 subjects at a fixed distance, and a subject varying the location. We examined the vital signs in the selected range bin, and evaluated their accuracy in terms of the mean error and the correctness. The results show that the proposed range bin selection method performs better than the conventional methods.

REFERENCES

- [1] A. Anghel, G. Vasile, R. Cacoveanu, C. Ioana, and S. Ciocchina, "Short-range wideband FMCW radar for millimetric displacement measurements," *IEEE Trans. Geosci. Remote Sens.*, vol. 52, no. 9, pp. 5633–5642, Sep. 2014.
- [2] M. He, Y. Nian, and Y. Gong, "Novel signal processing method for vital sign monitoring using FMCW radar," *Biomed. Signal Process. Control*, vol. 33, pp. 335–345, Mar. 2017.
- [3] L. Anitori, A. de Jong, and F. Nennie, "FMCW radar for life-sign detection," in *Proc. IEEE Radar Conf.*, Dec. 2009, pp. 1–6.
- [4] C. Li, M.-R. Tofghi, D. Schreurs, and T.-S. J. Horng, *Principles and Applications of RF/microwave in Healthcare and Biosensing*. New York, NY, USA: Academic, 2016.

- [5] P. E. Pace, *Detecting and Classifying Low Probability of Intercept Radar*. Norwood, MA, USA: Artech House, 2009.
- [6] H. Song and H.-C. Shin, "Classification and spectral mapping of stationary and moving objects in road environments using FMCW radar," *IEEE Access*, vol. 8, pp. 22955–22963, 2020.
- [7] S. Lee, B.-H. Lee, J.-E. Lee, and S.-C. Kim, "Statistical characteristic-based road structure recognition in automotive FMCW radar systems," *IEEE Trans. Intell. Transp. Syst.*, vol. 20, no. 7, pp. 2418–2429, Jul. 2019.
- [8] B. Dekker, S. Jacobs, A. S. Kossen, M. C. Kruithof, A. G. Huizing, and M. Geurts, "Gesture recognition with a low power FMCW radar and a deep convolutional neural network," in *Proc. Eur. Radar Conf. (EURAD)*, Oct. 2017, pp. 163–166.
- [9] Z. Zhang, Z. Tian, and M. Zhou, "Latern: Dynamic continuous hand gesture recognition using FMCW radar sensor," *IEEE Sensors J.*, vol. 18, no. 8, pp. 3278–3289, Apr. 2018.
- [10] C. Li, W. Chen, G. Liu, R. Yan, H. Xu, and Y. Qi, "A noncontact FMCW radar sensor for displacement measurement in structural health monitoring," *Sensors*, vol. 15, no. 4, pp. 7412–7433, Mar. 2015.
- [11] G. Wang, C. Gu, J. Rice, T. Inoue, and C. Li, "Highly accurate noncontact water level monitoring using continuous-wave Doppler radar," in *Proc. IEEE Topical Conf. Wireless Sensors Sensor Netw. (WiSNet)*, Jan. 2013, pp. 19–21.
- [12] Y. Tokieda, H. Sugawara, S. Niimura, and T. Fujise, "High precision waterlevel gauge with an FMCW radar under limited bandwidth," in *Proc. Eur. Radar Conf.*, 2005, pp. 339–342.
- [13] H. Lee, B.-H. Kim, J.-K. Park, S. W. Kim, and J.-G. Yook, "A resolution enhancement technique for remote monitoring of the vital signs of multiple subjects using a 24 GHz bandwidth-limited FMCW radar," *IEEE Access*, vol. 8, pp. 1240–1248, 2020.
- [14] G. Wang, J.-M. Munoz-Ferreras, C. Gu, C. Li, and R. Gomez-Garcia, "Application of Linear-Frequency-Modulated continuous-wave (LFMCW) radars for tracking of vital signs," *IEEE Trans. Microw. Theory Techn.*, vol. 62, no. 6, pp. 1387–1399, Jun. 2014.
- [15] J.-M. Munoz-Ferreras, J. Wang, Z. Peng, C. Li, and R. Gomez-Garcia, "FMCW-Radar-Based vital-sign monitoring of multiple patients," in *Proc. IEEE MTT-S Int. Microw. Biomed. Conf. (IMBioC)*, May 2019, pp. 1–3.
- [16] M. Alizadeh, G. Shaker, J. C. M. De Almeida, P. P. Morita, and S. Safavi-Naeini, "Remote monitoring of human vital signs using mm-wave FMCW radar," *IEEE Access*, vol. 7, pp. 54958–54968, 2019.
- [17] H. Lee, B.-H. Kim, J.-K. Park, and J.-G. Yook, "A novel vital-sign sensing algorithm for multiple subjects based on 24-GHz FMCW Doppler radar," *Remote Sens.*, vol. 11, no. 10, p. 1237, May 2019.
- [18] O. Postolache, P. Girao, E. Pinheiro, R. Madeira, J. M. D. Pereira, J. Mendes, G. Postolache, and C. Moura, "Multi-usage of microwave Doppler radar in pervasive healthcare systems for elderly," in *Proc. IEEE Int. Instrum. Meas. Technol. Conf.*, May 2011, pp. 1–5.
- [19] S. Schafer, A. R. Diewald, D. Schmiech, and S. Muller, "One-dimensional patch array for microwave-based vital sign monitoring of elderly people," in *Proc. 19th Int. Radar Symp. (IRS)*, Jun. 2018, pp. 1–10.
- [20] G. Fedele, E. Pittella, S. Pisa, M. Cavagnaro, R. Canali, and M. Biagi, "Sleep-apnea detection with UWB active sensors," in *Proc. IEEE Int. Conf. Ubiquitous Wireless Broadband (ICUWB)*, Oct. 2015, pp. 1–5.
- [21] A. Ahmad, J. C. Roh, D. Wang, and A. Dubey, "Vital signs monitoring of multiple people using a FMCW millimeter-wave sensor," in *Proc. IEEE Radar Conf.*, Apr. 2018, pp. 1450–1455.
- [22] C. Li, J. Cummings, J. Lam, E. Graves, and W. Wu, "Radar remote monitoring of vital signs," *IEEE Microw. Mag.*, vol. 10, no. 1, pp. 47–56, Feb. 2009.
- [23] J.-Y. Park, Y. Lee, Y.-W. Choi, R. Heo, H.-K. Park, S.-H. Cho, S. H. Cho, and Y.-H. Lim, "Preclinical evaluation of a noncontact simultaneous monitoring method for respiration and carotid pulsation using impulse-radio ultra-wideband radar," *Sci. Rep.*, vol. 9, no. 1, Dec. 2019, Art. no. 11892.
- [24] M. Jankiraman, *FMCW Radar Design*. Norwood, MA, USA: Artech House, 2018.
- [25] K. Mostov, E. Liptsen, and R. Bouthcko, "Medical applications of short-wave FM radar: Remote monitoring of cardiac and respiratory motion," *Med. Phys.*, vol. 37, no. 3, pp. 1332–1338, Mar. 2010.
- [26] A. Jeffrey and D. Zwillinger, *Table Integrals, Series, Products*. Amsterdam, The Netherlands: Elsevier, 2007.
- [27] Bitsensing. Accessed: Oct. 7, 2020. [Online]. Available: http://bitsensing.com/pdf/Technical_Specification_InCabinRadar_miniV.pdf
- [28] G. Wang, C. Gu, T. Inoue, and C. Li, "A hybrid FMCW-interferometry radar for indoor precise positioning and versatile life activity monitoring," *IEEE Trans. Microw. Theory Techn.*, vol. 62, no. 11, pp. 2812–2822, Nov. 2014.
- [29] D. Model, *Making Sense of Clinical Examination of the Adult Patient: Hands-on Guide*. Boca Raton, FL, USA: CRC Press, 2006.
- [30] A. Taktak, P. Ganney, D. Long, and R. Axell, *Clinical Engineering: A Handbook for Clinical and Biomedical Engineers*. New York, NY, USA: Academic, 2019.
- [31] C. Li, V. M. Lubecke, O. Boric-Lubecke, and J. Lin, "A review on recent advances in Doppler radar sensors for noncontact healthcare monitoring," *IEEE Trans. Microw. Theory Techn.*, vol. 61, no. 5, pp. 2046–2060, May 2013.
- [32] M. S. Woolfson, "Study of cardiac arrhythmia using zero-crossing analysis," *J. Biomed. Eng.*, vol. 11, no. 4, pp. 303–310, Jul. 1989.
- [33] V. L. Petrović, M. M. Janković, A. V. Lupšić, V. R. Mihajlović, and J. S. Popović-Božović, "High-accuracy real-time monitoring of heart rate variability using 24 GHz continuous-wave Doppler radar," *IEEE Access*, vol. 7, pp. 74721–74733, 2019.



HO-IK CHOI received the B.S. degree in electrical engineering from the Pohang University of Science and Technology (POSTECH), Pohang, South Korea, in 2016, where he is currently pursuing the Ph.D. degree in electrical engineering.

Since 2016, he has been a Research Assistant with the Department of Electrical Engineering, POSTECH. His research interests include bio signal processing and radar signal processing.



HEEMANG SONG (Member, IEEE) received the B.S. degree in electronic engineering from Soongsil University, Seoul, South Korea, in 2015, where he is currently pursuing the Ph.D. degree. Since 2015, he has been a Research Assistant with the Department of Electronic Engineering, Soongsil University. His research interest includes radar signal processing focusing on automobile.



HYUN-CHOOL SHIN (Member, IEEE) received the M.Sc. and Ph.D. degrees in electronic and electrical engineering from the Pohang University of Science and Technology (POSTECH), South Korea, in 1999 and 2004, respectively.

From 2004 to 2007, he was a Postdoctoral Researcher with the Department of Biomedical Engineering, School of Medicine, Johns Hopkins University. Since 2007, he has been a Professor of electronic engineering with Soongsil University.

His research interests include neural engineering and neural signal processing focusing on brain-machine interface, brain injury detection, and radar signal processing for biomedical applications.